http://ijopaar.com; 2016 Vol. 4(1); pp. 08-17.

Investigations on Growth, structural, mechanical and conductivityMeasurements of Nitric acid (HNO_3) doped Triglycine Phosphate (TGP) Single Crystals for NLO applications

M. R. Meera[a,b], S. L. Rayar[c], V. BenaJothy[a,*]

[a]Department of Physics and Research Centre, Women's Christian College, Nagercoil, Tamil Nadu, India, 629 001.

[b]Department of Physics, Sree Ayyappa College for Women,Chunkankadai., Nagercoil, Tamil Nadu, India, 629807.

[c]Department of Physics, St. Judes College,Thoothoor, Tamil Nadu. India

Email: meeranairmrm17@gmail.com

Date of revised paper submission: 10/12/2016; Date of acceptance: 20/12/2016
Date of publication: 29/12/2016; *First Author / Corresponding Author; Paper ID: A16404.
Reviewers: Dr. B. B. Srivastava, India; Dr. A. K. Soni, India.

Abstract

Single crystals of ferroelectric material triglycine phosphate (TGP) have been grown by slow evaporation method. The effect of Nitric acid (HNO_3) addition on the growth of TGP crystal has been studied for various concentrations (0.25, 0.50, 0.75 and 1.0 mol %). Solubility of the grown samples was found to be increasing with increase in temperature. The grown TGP crystal is observed to be crystallizing in monoclinic structure. Functional groups present in the grown pure and HNO_3 doped TGP crystals were confirmed from the vibrational frequencies of recorded FTIR and FT-Raman spectra. Kurtz–Perry powder technique was used to check the nonlinear optical activity of the pure andHNO_3 doped TGP crystals. Physical properties such as conductivity and mechanical studies have been performed for the pure and HNO_3 doped TSP crystals. The obtained results are presented and discussed.

Keywords: Growth from solution; FT-IR, Raman spectra; Microhardness, SHG efficiency, Dc conductivity.

1. Introduction

Advancement of laser and laser technology is one of the landmark achievements in scientific research in the 20th century. Especially in the research related to matter, its nature and interaction of same with light have been experimented in hundreds of novel methodology by using the laser technology. Such studies have resulted in finding several new optical phenomena of which the development in the field of nonlinear optics needs special mentioning of. In the later stages such studies have leaned towards research in the semiorganic materials because of the higher mechanical strength and Chemical stability [1].Their high SHG efficiency linked to the above characteristic make them the best option for nonlinear applications. Amino acids offer big non linearity and promising optical properties due to it possesses proton donor amine group (NH_3^+) and proton accepter carboxyl group (COO_2^-). Such zwitterionic nature attributing to crystals hardness is the most required quality for application in NLO devices. Efforts on synthesizing of amino acid mixed organic – inorganic complex crystals is being undertaken currently in an attempt to reach higher chemical stability , laser damage threshold linear and nonlinear optical properties [2–7]. In research related to amino acids glycine family crystals are identified for their better NLO properties [8-11]. Glycine exists as dipolar ions in which the carboxyl group is present as a carboxylate ion and the amino group as ammonium ion .The higher melting point attributes to its dipolar nature. Glycine and its methylated analogues

form complexes with mineral acids exhibiting interesting physical properties like ferroelastic, ferroelectric or anti ferroelectric behaviour [12]. Doping of NLO crystals with organic impurities is found as altering their physical and chemical properties to enhance their possibility of their usage in the optoelectronic devices [13–16]. Many of the additives cause habit modification, but do not effect significant changes in properties [17]. It is reported that substitution phosphorus for sulfur in the TGS structure has found to have influenced marginally the spontaneous polarization of the TGS [18]. Substitution of phosphate in the TGS crystal leads to increase in Tc, i.e., 52.5 ◦C [19]. In the present work nitric acid is used as dopant in the TGP crystals. It is reported that nitrate ions play a significant l role in the spontaneous polarization of the DGN crystal [20] Nitric acid is expected to increase dielectric constant and Tc due to its intrinsic dipole moment. The objective of the present work is to investigate the effect of HNO_3 addition on the growth, spectral, thermal, dielectric and mechanical properties of TGP crystals.

2. Experimental Details

2.1. Material Synthesis and Preparation

The parent compound TGP has been synthesised by dissolving Analar grade of glycine and phosphoric acid in double distilled deionised water with stiochiometric ratio of 3:1 according to the reaction:

$$3(NH_2CH_2COOH) + H_3PO_4 \rightarrow (NH_3CH_2COOH)_3.\ PO_4.$$

For minimizing impurity content in the TGP successive recrystallization is used. The pH value of the saturated solution of TGP was found to be 2.48. As the solubility of pure and nitric acid added TGP in double distilled water were determined at various temperatures because the growth rate of a crystal depends on solubility and growth temperature and is shown in Fig. 1.The solubility of HNO_3admixtured TGP is slightly higher than that of pure TGP. The solubility can be improved with the use of compatible acids as it's, a fact ascertained in the previous studies. In either case, ie., pure and doped crystals, positive slope of the solubility curve enables growth by either slow cooling or slow evaporation; in the present work slow evaporation method is used .

The final solution is subjected to filtering by filter papers and thereafter kept in beakers covered with perforated sheets. The solvent evaporation process for 15-20 days results super saturation enabling growth of transparent crystals with maximum possible dimension. In case of nitric acid added TGP solution, the pH values increased with increase in nitric acid concentrations (0.25, 0.50, 0.75 and 1.0mol%) : 2.50, 2.54,2.57 and 2.58 respectively. Here, the crystal growth began after 3 days of solvent evaporation and attained the maximum size in about 15-20 days and photographs of the grown crystals (pure and HNO_3doped TGP) were shown in Figure 2. The grown crystals were carefully harvested and then subjected to the following characterization studies.

2.2. Characterization

Enraf nonius-cad4 diffractometer is used for carrying out the process of single crystal X-ray diffraction. FT-IR spectra of pure and HNO_3 doped TGP have been recorded using Bruker IFS 66 V Spectrometer in the range 4000-100 cm^{-1}. FT Raman spectra were recorded using Bruker RFS 27: Stand alone FT-Raman Spectrometer with resolution of 2 cm^{-1}.Microhardness analysis was carried out using vicker's micro hardness indentor. Q-Swiched High Energy Nd:YAG Laser (QUANTA RAY MODEL) HG-4B-High efficiency instrument was used to carry out for the recording of SHG measurement. Dielectric studies of the grown crystals were carried out to an accuracy of $\pm 1^{o}C$ using a megohmmeter with various temperatures ranging from $30^{o}C$ to $150^{o}C$.

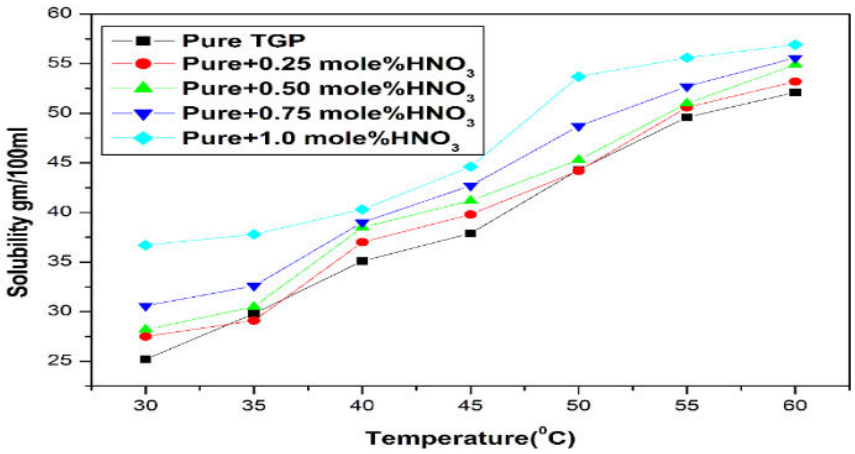

Figure1: Solubility curve of pure and HNO_3 admixtured TGP

Figure 2: Photographs of the grown crystals (pure and 0.25, 0.50, 0.75 and 1.0 mol% HNO_3 doped TGP)

3. Result and Discussion

3.1. Single Crystal XRD

Single crystal XRD has been carried out using Enraf nonius-cad4 diffractometer. The data obtained show that the grown crystal of Triglycine phosphate crystal belongs to monoclinic system with lattice parameters a = 5.094 Å, b= 11.984 Å, c = 5.453 Å, $\alpha = \gamma = 90°$ and $\beta = 111.70°$.

3.2. Vibrational Analysis

To confirm the presence of nitric acid in TGP and to analyze qualitatively the presence of the functional groups in the grown crystals, the FTIR spectra of pure and 0.25, 0.50, 0.75 and 1.0mol % HNO_3 doped TGP were recorded. The FTIR spectra and Raman of pure and 0.25, 0.50, 0.75 and 1.0mol % HNO_3 doped TGP are shown in figures 3(a) and 3(b) and the vibrational assignments were given in Table 1. The nitrate anion in nitric acid is a potential acceptor and thus N-H...O hydrogen bonds may be formed [21]. As such, O atom is an acceptor of protons and accepts a proton. The nitrogen/oxygen stretch of nitrate appears as an intense band between 1400 and 1340 cm^{-1}. Generally, symmetric and symmetric NO_3^- ions occur in the region 1300-1550 and 700-751 cm^{-1}[22]. The bands at ~1399 cm^{-1} and 792 cm^{-1} in IR spectra are more reasonably assignable to asymmetric and symmetric NO_3^- ion. OH stretching mode is observed at ~3330 cm^{-1}. Its absence in the pure TGP spectrum and its presence in the doped TGP spectra clearly indicate the presence of nitric acid in the lattice of TGP crystal. P-O stretching vibrations are expected in the region 1040-910 cm^{-1} [23] which is observed in IR at ~1042 cm^{-1}. S=O stretching mode is observed at ~1390 cm^{-1}. C=O stretching vibrations in the ketones, saturated aliphatic aldehydes and acids have frequencies in range of 1740–1700 cm^{-1}. In amides the frequency is lowered to 1690 cm^{-1} [24] which is due to existence of resonance structures. C=O stretching band is observed at 1590 cm^{-1}. The deformation vibration of the carboxylate ion is observed at 682.95 cm^{-1}. C=O and NH_2 stretching vibrations are shifted and strongly evidences of intra-molecular interactions.

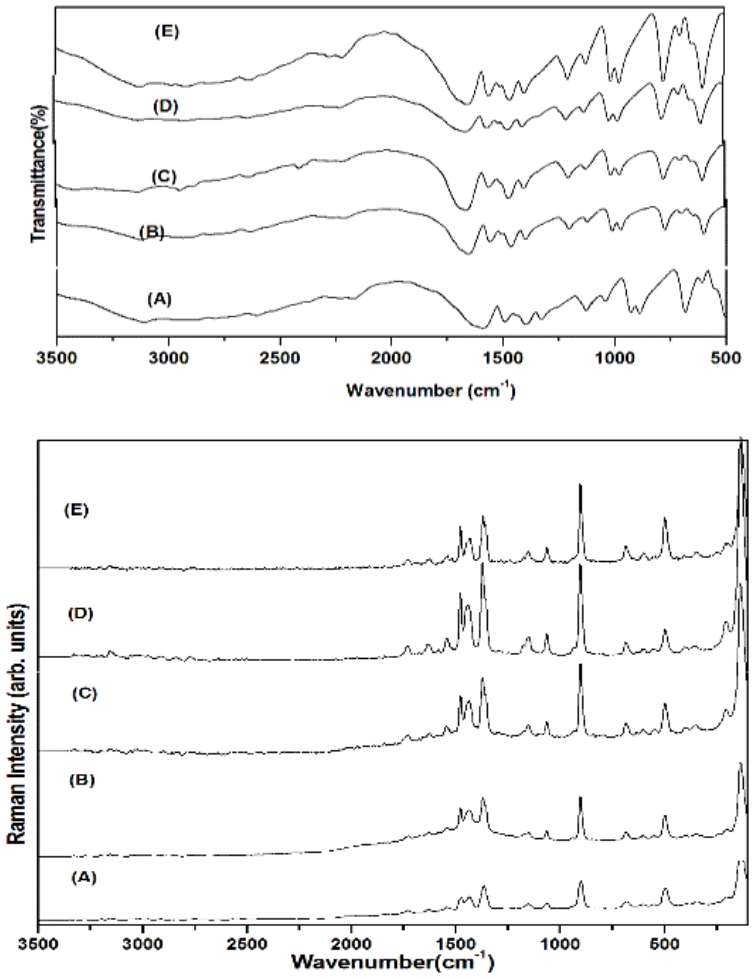

Figure 3(a) FT IR and (b) FT Raman Spectra

(A) Pure TGP **(B)** TGP + 0.25mol % of HNO_3 **(C)** TGP + 0.50 mol % of HNO_3 **(D)** TGP + 0.75mol % of HNO_3 **(E)** TGP + 1.0 mol % of HNO_3

Table 1 Vibrational assignments of pure and HNO_3 doped TGP crystal

Pure TGP (cm^{-1})		**TGP Doped with HNO_3(cm^{-1})**								**Assign ments**
		0.25 mole%		**0.50 mole%**		**0.75mole%**		**1.0 mole%**		
		IR	**Raman**	**IR**	**Raman**	**IR**	**Raman**	**IR**	**Raman**	
			3336		3330		3333		3324	νOH
			3272		3272		3270		3249	νNH
			3196	3408	3203		3205		3199	νNH
3110	3156	3109	3145			3107	3155	3109	3161	$\nu_{as}NH_2$
2962		2962		2924		2963		2963		$\nu_{ss}NH_2$
2890	2920	2918	2901		2912	2892	2912	2888	2912	νCH_2
2792		2792				2792		2791		νCH_2

2605		2605		2606		2604		2604		νCH_2
	1730		1721		1728		1730		1730	νC=O
	1628		1623		1628		1624		1624	νC=O
1590	1542	1595		1596	1586	1594	1584	1593	1584	νC=O
			1542		1542		1542		1542	$\nu_{as}NO_3^-$
1490	1472	1492	1473	1491	1473	1492	1476	1491	1476	βNH_2, βOH
		1437	1433		1433	1439	1442	1438	1442	βNO_3^-
		1397		1399		1395		1393		$\nu_{ss}NO_3^-$
1395	1362		1369		1369		1370		1370	$\nu_{ss}COO^-$,
1326		1328		1328		1327		1327		νP=O,
1125	1154	1125	1150	1124	1152	1125	1152	1125	1152	νP=O
1041	1062	1041	1064	1041	1064	1041	1062	1041	1062	νP- O
926		927		927		927		927		defCO O
887	898	888	908	888	908	888	902	888	902	υ (C-C)
					792					δ OH
	682	684	684	683	686	683	686	683	686	νHCl
					634					δNO_3
607	604	607	597	608	604	607	604	608	604	δ(C-N)
501		503	500	502		502		501		ρ (COO^-)

v-stretching; v_{as}-asymmetric stretching; v_{ss}-symmetric stretching; β=- Bending; def=deformation

3.3. Micro Hardness Analysis

In order to ascertain fracture behaviour, yield strength, brittleness index and temperature of cracking, microhardness testing is used, being the well-known method for studying the mechanical properties [25]. Transparent, pure and nitric acid added TGP crystals devoid of any cracks were separated and subjected to hardness measurement to ascertain their resistance to local deformation. Vickers microhardness measurements were carried out using vicker's microhardness indentor. Fine polished crystals of different magnitudes (25, 50 and 100 g) were placed on the platform of the microhardness and the loads were applied over a fixed interval of time. Vickers hardness number (H_v) of the crystals is calculated using the relation

$$H_v = 1.8544\ (P/d^2)\ kg/mm^2$$

Where P is the indentor load in kg, d is the diagonal length of the impression in mm and 1.8544 is a constant [26].The hardness number (H_v) with applied load (g) detected for the pure and HNO_3 admixtured TGP crystals is shown in Fig. 4a. The results show hardness value increases with the applied load. The reason for lower value of hardness at the lower loads is the reduction in the strength of the surface layers due to surface moisture absorption occurring surface by surface. As shown in Fig 4a.hardness value increases rapidly on increase of applied load (25, 50, and 100 g). Cracks developed on the surface as the hardness value increases above 100 g because of the release of internal stresses generated locally by indentation. Applied load below 100 g. is suggested for device fabrication purpose. The increasing of hardness with increasing load is the reverse indentation size effect (RISE).For analysing of the RISE experimentally Meyer's law is used [27], by correlating the applied load P with the corresponding indentation size (d) by the relation P = Ad, where n is the Meyers index or work hardening exponent and A is a constant. The plot obtained between log P and log d gives a straight line which is shown in Fig 4b. The work hardening coefficient (n) calculated from Fig. 4b by the least square fit method and is shown in Table 2. According to Onitsch [28], if the value of n exists between 1 and 1.6 it refers to hard materials and for soft materials it is above 1.6.

Since n values of the pure and HNO_3admixtured TGP crystals were above 1.6, all grown crystals belong to the category of soft materials.

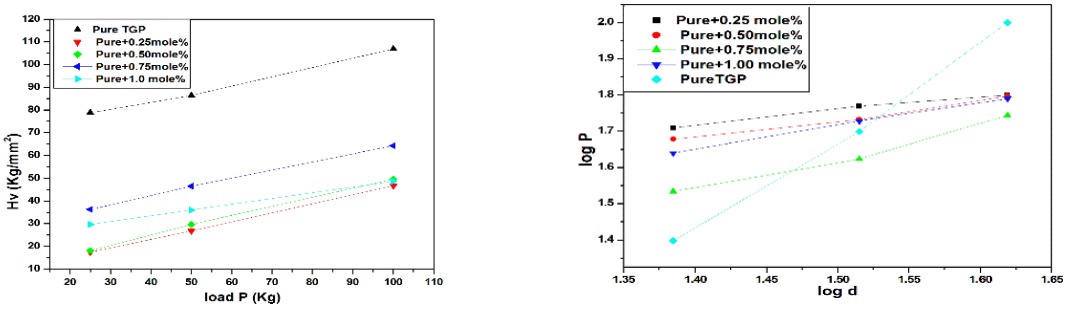

Figure 4 (a) Variation of Hv with load P **(b)** Plot of log d versus log p of Pure and H_2SO_4 doped TGP crystals

Table 2 Values of work hardening coefficient (n) for pure andHNO_3admixtured TGP crystals

Samples	Work hardening coefficient (n)
Pure TGP crystal	2.5575
TGP + 0.25mol % of HNO_3	4.38128
TGP + 0.50 mol % of HNO_3	2.76265
TGP + 0.75mol % of HNO_3	2.58488
TGP + 1.0 mol % of HNO_3	4.05018

3.4. Non Linear Optical Studies

To study the transferring energy from fundamental beam to second harmonic beam, Second Harmonic Generation (SHG) efficiency of a nonlinear optical material is analyzed. For the initial screening of materials for second harmonic generation (SHG) and identification as non-centro symmetric crystal structure, Kurtz and Perry [29] powder technique is utilized. A second harmonic signal of 11.82mV,10.78 mV,7.68 mV,10.29 mV, and 7.63mV were obtained from pure and HNO_3(0.25,.50,0.75 and 1.0 mole %) doped TGP respectively, with reference to 17.3mV of KDP. Thus, the SHG efficiency of pure TGP is roughly 0.69 times that of KDP. In the present work it is concluded that in the doped samples the SHG efficiency is reduced and the reason for such reduction is due to the deterioration of crystalline perfection. Such deterioration is resulted from disturbance of charge transfer in the sample due to incorporation of nitrate ions. The ascertainment of SHG efficiency of the samples of present work indicates them as better candidates for NLO applications.

3.5. Dc Conductivity Studies

Proton transport within the framework of hydrogen bonds affects electrical conductivity. Impurities into the crystal lattice and corresponding defects in ionic crystals are directly associated with conductivity [30-32]. The proton conduction is due the motion of protons accompanied by a D defect (excess of positive charge). There may not be any change in the charge at electrode due to migration but there may be electric polarization. Conductivity is regulated by chemical composition, purity and crystal structure of the material.

Therefore evaluation of DC electrical conductivity gives important information about the materials to exploit them for the various applications. The Gibb's free energy of a crystal is minimum at any particular temperature, when a certain fraction of ions leave the normal lattice. To measure DC conductivity of the grown crystals two-probe technique is employed. Samples polished with silicon carbide paper obtained after cutting (rectangular shaped crystals) parallel to the cleavage plane to the desired thickness of 1-2 mm. To obtain a good ohmic contact with the electrodes,

opposite faces of the crystals were coated with good quality graphite. The resistance of the crystals was measured using a megohmmeter. The observations were made while cooling the sample and temperature was controlled to an accuracy of order up to ± 1°C.The dimensions of crystal were measured with the help of travelling microscope. The DC conductivity (σ_{dc}) of the crystal was calculated using the relation,

$$\sigma_{dc} = d/RA$$

Where R denotes the measured resistance, d denotes the thickness of the sample and A is the area of face in contact with the electrode. DC conductivity value is found to increase proportionately with temperature, which indicates the temperature dependence activation energy (E_{dc}) and it is a characteristic of small polaron hopping (SPH) conduction mechanism. There is a possibility of weakening of the hydrogen bonding system due to rotation of the carboxyl ions in the glycine molecules, when the temperature of the crystal is increased.

In the present study increase of conductivity along with increase of temperature observed for the pure and HNO_3 added TGP crystals may be due to the temperature dependence of the proton transport. And also it is clear that dc electrical conductivity is not varying with the impurity concentration in the solution used for the growth of single crystals. The replacement of phosphate ions by nitrate ions in the interstitial positions may create a disturbance in the hydrogen bonding system at random and may cause the electrical parameters vary nonlinearly with the impurity concentration. Dc conductivity Vs temperature graph is shown in Fig. 5. The graph explains the increase in the conductivity with the increase in the temperature due to the increase in mobility and release of ions at elevated temperatures.

The general relation for the temperature variation of conductivity is given by

$$\sigma_{dc} = \sigma_0 \exp[-E_a/kT]$$

Where σ_0 is a constant depending on material, E is the activation energy, T the absolute temperature and k isthe Boltzmann's constant. The above equation can be rewritten as

$$\ln\sigma_{dc} = \ln\sigma_0 - E_a/kT$$

A plot of ln σ_{dc} versus 1000/T[Fig 6] gives - E/k as the slope and ln σ_{dc} as the intercept. It is customary to plot ln σ_{dc} versus 1000/T, from the slope of which activation energy (E) can be calculated and it is found to be 0.498eV,0.475eV,0.378eV,0.416eV and 0.405 eV for the crystals of pure and (0.25,0.50,0.75 and 1.0 mol %)H_2SO_4 doped TGP. The grown crystals have the activation energy value which is more than reported value of KDP (0.22eV). The obtained activation energy values shows that all the grown crystals are non-semiconducting in nature. A similar range of Activation energy values have been reported for some super- ionic conductors [33].

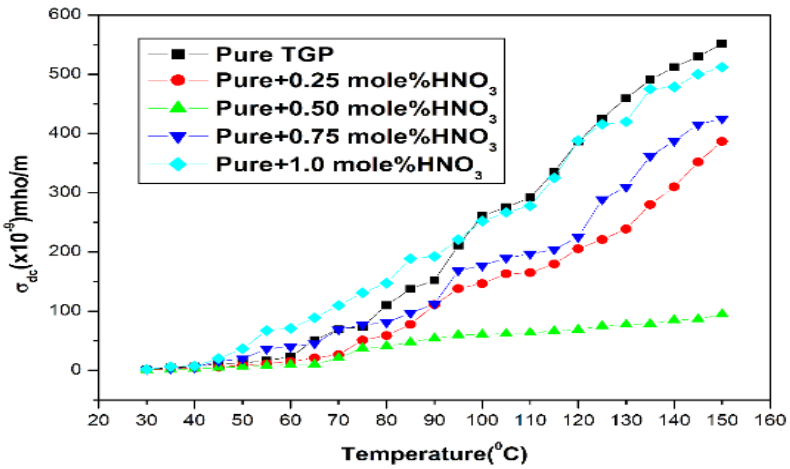

Fig 5: Variation of σ_{dc} with Temperature for Pure and HNO_3 doped TGP crystals

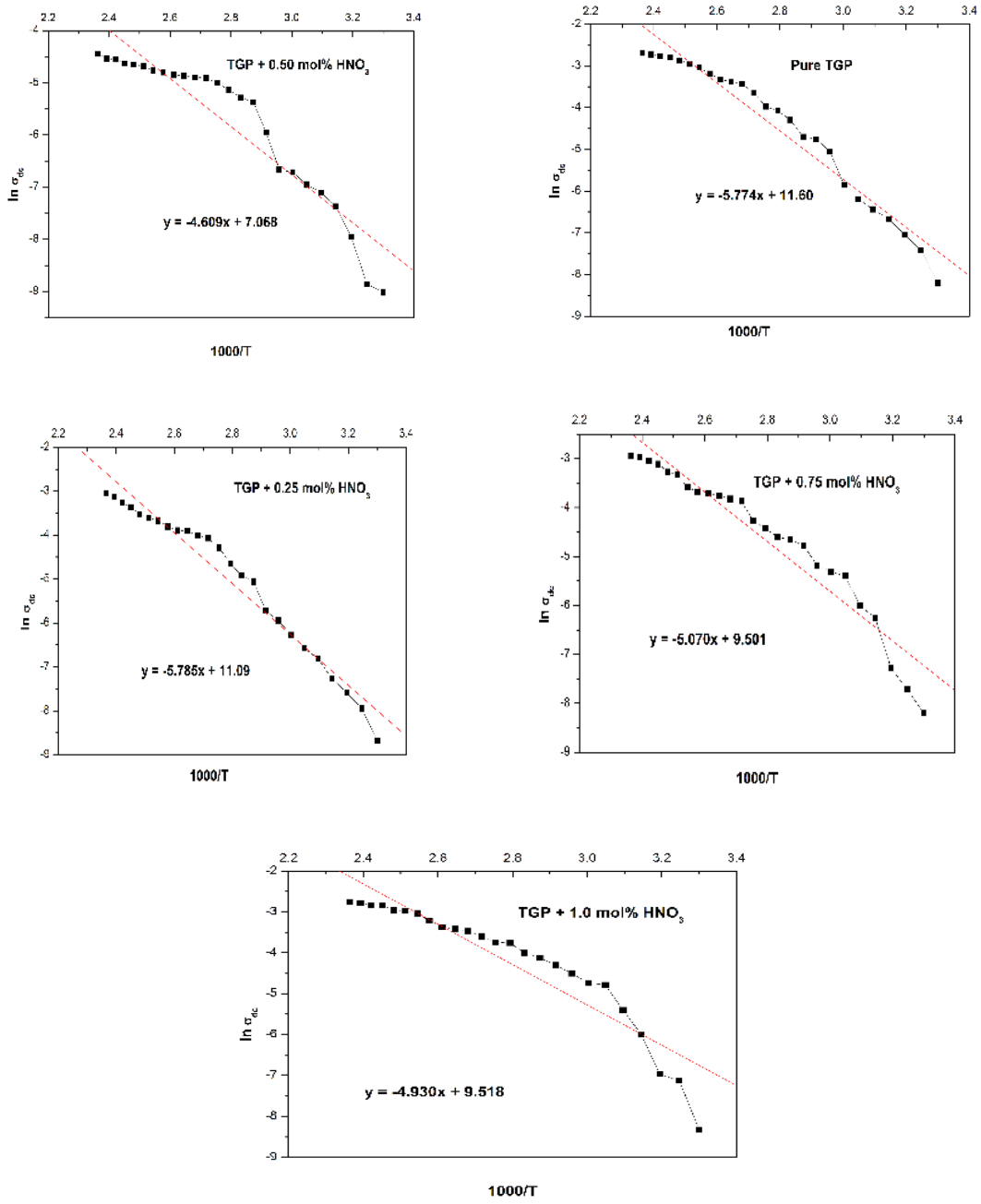

Figure 6. Plot of ln σ_{dc} versus 1000/T for Pure and nitric acid (HNO_3) added TGP single crystal

4. Conclusion

Pure and HNO_3 doped (0.25, 0.50, 0.75 and 1.0 mol % concentrations) TGP crystals have been successfully grown by the free evaporation method. The monoclinic crystal system of the grown crystals was identified by SXRD analysis. that The presence of zwitter and glycinium ions in both pure and HNO_3 doped crystals were strongly suggested by the spectral investigations by IR and Raman spectroscopy and also FTIR spectra shows that glycine molecule exists as a dipolar ion in which the carboxyl group present as carboxylate ion and amino group present as ammonium ion.

Microhardness analysis reveals that all the grown crystals belongs to the category of soft materials. The property of SHG studies reveals that the grown crystals are a better material for NLO applications. All the five crystals grown are found to exhibit normal dielectric behaviour. The Arrhenius plot confirms that the activation energy which infers that all the grown crystals will act in between super-ionic conductor and dielectric.

Acknowledgement

The author (M. R. Meera) is grateful to the University Grants Commission (UGC), Government of India for the award of a Teacher Fellowship under FDP scheme leading to the Ph.D. degree.

References

1. Xu, D., Jiang, M. and Tan, Z., 1983, Acta.Chem. Sin. 41, 570.
2. Monaco, S. B., Davis, L. E., Velsko, S. P., Wang, F. T., Eimerl, D., Zalkin, A., 1987, J. Cryst., Growth85, 252–255.
3. Pal, T., Kar, T., Wang, X. Q., Zhou, G. Y., Wang, D., Cheng, X. F., Yang, Z. H., 2002, J. Cryst. Growth 235, 523–528.
4. Pal, T. Kar, T., Bocelli, G., Rigi, L., 2003, Cryst. Growth Des.3, 3–16.
5. Mohan K. R., Rajan Babu, D., Jayaraman, D., Jayavel, R., Kitamura, K., 2005, J. Cryst. Growth 275, e-1935–e-1939.
6. Narayan Bhat, M., Dharmaprakash, S. M., 2002, J. Cryst. Growth 236, 376–380.
7. Kandasamy, A., Siddeswaran, R., Murugakoothan, P., Suresh Kumar, P., Mohan, R., 2007, Cryst. Growth Des.7, 183–186.
8. Albert L. Lehninger, 1984, Principles of Biochemistry, CBS Publishers, New Delhi.
9. Marsh, R. E., 1958, Acta Crystallogr., 11, 654.
10. Iitaka, Y., 1960, Acta. Crystallogr., 13, 35.
11. Iitaka, Y., 1961, Acta. Crystallogr., 14, 1.
12. Ambujam, K., Rajarajan, K., Selvakumar, S., Madhavan, J., Gulam Mohamed, Sagayaraj, P., 2007, Opt. Mater. 29, 657–662.
13. Krishnan, C.; Selvarajan, P.; Freeda, T. H., 2008, J. Crystal Growth, 311 (1), 141–146.
14. John, N. J., Selvarajan, P., Benita Jeba Silviya, Mahadevan, S., 2007, Mater. Manufact. Process, 22 (3), 379–383.
15. Rajarajan, K., Ginson, P., Ravikumar, S., VethaPotheher, I., Pragasam, J. A., Ambujam, K. Sagayaraj, 2007, Mater. Manufact. Process, 22 (3), 370–374.
16. Praveen, V. N., Vijayan, N., Mahadevan, C. K., Ghagavannarayana, G., 2008, Mater. Manufact. Process, 23 (8), 816–822.
17. Gaffar, M. A., Abu El Fadl, A., Mansor, S. A., 1989, J. Phys. D: Appl. Phys. 22, 327.
18. Fang, C. S., Xi, Y., Chen, Z. X., Bhalla, A. S., Cross, L. E., 1983, Mater. Lett.2, 8.
19. Mohan Kumar, R., Muralidharan, R., Rajan Babu, D., Rajendran, K. V., Jayavel, R., Jayaraman, D., Ramasamy, P., 2001, J. Cryst. Growth 229, 568.
20. Sato, S., 1968, J. Phys. Soc. Jpn. 25, 185.
21. Krishnakumar, R. V., SubhaNandhini, M., Natarajan, S., Sivakumar, K., Babu Varghese, 2001, Acta Crystallogr, C57, 1149.
22. Nyquist, R. A., Putzig, C. L., Leugers, M. A., 1995, Infrared and Raman Spectral Atlas of Inorganic Compounds and Organic Salts, Academic press, New York.
23. Smith, B. C., 1999, Infrared Spectral Interpretation, A Systematic Approach, CRC Press, Washington, DC.
24. Socrates, G., 1980, Infrared Characteristic Group Frequencies, Wiley-Interscience Publication.
25. Raina, U., Bhat, S., Wanklyn, B. M., Kotru, P. N., 1993, Mater. Chem. Phys. 34, 257–262.
26. Rajesh, N. P., Kannan, V., Santhana Raghavan, P., Ramasamy, P., Lan, C. W., 2002, Mater. Lett.52, 326–328.
27. Meyer, E., 1908, Z. Phys. 9, 66–74.

28. Onitsch, E. M., 1947, Mikroskopie 2, 131–151.
29. Kurtz, S. K., Perry, T. T., 1968, J. Appl. Phys. 39, 3798.
30. Deepa, G., Freeda, T. H. and Mahadevan, C., 2002, Indian J. Phys., A76, 369.
31. Priya, M., Padma, C. M., Freeda, T. H., Mahadevan, C., Balasingh, C., 2001, Bull. Mater. Sci., 24, 511.
32. Sancta, J. A., Sutha, A. G., Freeda, T. H., Mahadevan, C., Balasingh, C., 2001, Indian J. Phys. A75, 245.
33. Babu Reddy, J. N., Vanishri, S., Ganesh Kamath ,Suja Elizabeth , Bhat, H. L., Isakov, D., Belsley, M., deMatos Gomes, E., Aroso, T. L., 2009, J. Cryst. Growth 311, 4044–4049.